Materials Science in Semiconductor Processing 14 (2011) 139–145

Contents lists available at ScienceDirect

Materials Science in Semiconductor Processing

journal homepage: www.elsevier.com/locate/mssp

Temperature dependent current–voltage (I–V) characteristics of Au/n-Si (1 1 1) Schottky barrier diodes with PVA(Ni,Zn-doped) interfacial layer

Tuncay Tunç [a,*], Şemsettin Altindal [b], İbrahim Uslu [c], İlbilge Dökme [d], Habibe Uslu [b]

[a] Science Education Department, Faculty of Education, Aksaray University, Aksaray, Turkey
[b] Physics Department, Faculty of Arts and Sciences, Gazi University, Ankara, Turkey
[c] Chemistry Education Department, Faculty of Gazi Education, Gazi University, Ankara, Turkey
[d] Science Education Department, Faculty of Gazi Education, Gazi University, Ankara, Turkey

ARTICLE INFO

Article history:
Received 11 August 2010
Received in revised form
5 January 2011
Accepted 31 January 2011
Available online 23 February 2011

Keywords:
I–V–T characteristics
Barrier height
Gaussian distribution
Poly(vinyl alcohol)
Schottky barrier diodes
Electrospinning

ABSTRACT

Current–voltage (I–V) characteristics of Au/PVA/n-Si (1 1 1) Schottky barrier diodes (SBDs) have been investigated in the temperature range 80–400 K. Here, polyvinyl alcohol (PVA) has been used as interfacial layer between metal and semiconductor layers. The zero-bias barrier height (Φ_{B0}) and ideality factor (n) determined from the forward bias I–V characteristics were found strongly dependent on temperature. The forward bias semi-logarithmic I–V curves for different temperatures have an almost common cross-point at a certain bias voltage. The values of Φ_{B0} increase with the increasing temperature whereas those of n decrease. Therefore, we have attempted to draw Φ_{B0} vs. $q/2kT$ plot in order to obtain evidence of a Gaussian distribution (GD) of the barrier heights (BHs). The mean value of BH $\overline{\Phi}_{B0}$ and standard deviation (σ_0) were found to be 0.974 eV and 0.101 V from this plot, respectively. Thus, the slope and intercept of modified $\ln(I_0/T^2)-q^2\sigma_0^2/2(kT)^2$ vs. q/kT plot give the values of $\overline{\Phi}_{B0}$ and Richardson constant (A^*) as 0.966 eV and 118.75 A/cm^{2}K^2, respectively, without using the temperature coefficient of the BH. This value of A^* 118.75 A/cm^{2}K^2 is very close to the theoretical value of 120 A/cm^{2}K^2 for n-type Si. Hence, it has been concluded that the temperature dependence of the forward I–V characteristics of Au/PVA/n-Si (1 1 1) SBDs can be successfully explained on the basis of the Thermionic Emission (TE) theory with a GD of the BHs at Au/n-Si interface.

1. Introduction

A large number of metal/polymer/semiconductor Schottky barrier diodes (SBDs) have been prepared and characterized depending on the temperature and frequency in recent years [1–15]. There are many reports about conjugated conducting polymers in the area of electronics and optoelectronics. Among the various conducting polymers, poly(vinyl alcohol), polyaniline, poly (alkylthiophene), polypyrrole, polyophene and poly (3-hexylthiophene) have become an attractive research topic owing to their potential applications and interesting properties for chemists, physicists and electrical engineers alike [6–16]. With the existence of an interfacial layer, such as polyvinyl alcohol (PVA) or an insulator layer at metal/semiconductor interface, Schottky barrier heights (SBHs) are much more dependent on the metal work function [17,18] rather than other III–V materials, indicating a weaker pinning of Fermi level.

* Corresponding author. Tel.: +90 382 288 2258; fax: +90 382 2801180.
E-mail address: tctunc@gmail.com (T. Tunç).

1369-8001/$ - see front matter © 2011 Elsevier Ltd. All rights reserved.
doi:10.1016/j.mssp.2011.01.018

In general, electrical conductivity depends on the thermally generated carriers and the addition of suitable dopant materials. Therefore, to improve the electrical properties or conductivity of polymers, many physicists and chemists have focused on polymers doped with metal ions [19–24]. When a polymer is doped with metals especially transition elements such as Zn, Co, Ni, Cu, Fe in various quantities and forms, their incorporation within a polymeric system can be expected to enhance the conductivity of polymer [19–22]. On the other word, dopant material can induce modifications in the molecular structure and hence the microstructural property of the polymer. In particular the transition metal salts and nanoparticle-doped polymers are considered to be a new class of organic materials due to their considerable modification on physical properties, including microstructural, optical, electrical and thermal properties. These changes in physical properties, depend on the chemical nature of the dopant and the way in which they interact with the host polymer [23,24]. Especially, the reduction of leakage current and improvement of the electrical properties are essential for developing metal doped polymer based SBDs. PVA is an interesting synthetic polymer because it is water-soluble and industrially obtained by the alkaline hydrolysis of solutions of Poly(vinyl acetate) (PVAc), which are mainly due to hydrogen bonds between hydroxyl groups on the chain and water molecules or biomolecules [25]. PVA is a potential material having a very high dielectric strength (>1000 kV/mm), good charge storage capacity and dopant-dependent electrical and optical properties [26]. PVA is used as fibers, fibers mats, films, paper cloth, polymerization stabilizers, cements and mortars.

Due to above explanations, in this study, PVA film has been used as an interfacial layer between metal and semiconductor. PVA doped with different ratios of nickel (Ni) and zinc (Zn) has been produced and PVA(Ni,Zn-doped) nanofiber film on silicon semiconductor has been fabricated by the use of electrospinning technique.

Until now, both a complete description of current transport mechanism through barrier and understanding of the formation of Schottky barrier and insulator layer at M/S interface still remain a challenging problem. Furthermore, the change in temperature has important effects on the main diode parameters such as barrier height (Φ_{B0}), ideality factor (n), series resistance (R_s) and interface states (N_{ss}) [27–34]. The analysis of the forward bias I–V characteristics of the SBD measured only at room temperature does not give detailed information about the current-conduction mechanisms and the nature of the BH formed at M/S interface. On the other hand, when these measurements have been carried out at wide temperature range, they allow us to understand different aspects of current-conduction mechanism. Therefore, we have investigated the forward bias I–V characteristics of Au/ PVA(Ni,Zn-doped)/n-Si (1 1 1) SBDs in the wide temperature range of 80–400 K. Generally, the forward bias I–V characteristics are linear in the semi-logarithmic scale at low bias voltages but deviate from linearity due to the effect of R_s when the applied bias voltage is sufficiently large [35–40]. It has been often found that the values of Φ_{B0} extracted from the linear parts of semi-logarithmic I–V characteristics using TE theory increase with the increasing temperature while those of n decrease. These changes are more significant especially at low temperatures such that the behavior of Φ_{B0} and n cannot be explained in terms of the standard TE theory. The temperature dependent experimental analysis of the I–V data of metal–semiconductor (MS), metal–insulator–semiconductor (MIS) and metal–polymer–semiconductor structures is based on TE theory, and it usually exhibits an abnormal increase in Φ_{B0} values and a decrease in n values as the temperature is increased, which overall lead to non-linearity in the activation energy $\ln(I_0/T^2)$ vs. $1/T$ plot. The ideality factor, in general, is expected to be close to unity above room temperature. However, the current-conduction through inhomogeneous SBHs has been found to be characterized by the ideality factor that deviates significantly from unity [41]. The high values of ideality factor and barrier height have been attributed to interfacial layer (PVA), the image force lowering BH and particular distribution of interface states at M/S interface [17,18,42]. Recently, the nature and origin of the increase in the Φ_{B0} and a decrease in n with an increase in temperature in some studies have been successfully explained on the basis of a TE theory with a GD of the BHs [27–30,34–41]. According to this model, the pinch-off effect related to the interaction between adjacent regions with different barriers and the effective barrier are always lower than the mean value of the barrier distribution. Werner and Guttler [35] assumed that distribution of SBDs is a result of special inhomogeneities at the M/S interface. According to this model, the deviation of n from unity and its temperature depend on the barrier distribution. The parameter R_s is also effective especially in downward curvature region of the forward bias I–V characteristics.

In the previous study, we fabricated Au/PVA(Ni,Zn-doped)/n-Si Schottky diodes and temperature dependent electrical and dielectric properties of the diode were calculated from the capacitance–voltage (C–V) and conductance–voltage ($G/\omega-V$) measurements in the temperature range 80–400 K [43]. Therefore, in this study, to better interpret the experimental observed main electrical parameters such as n, Φ_{B0} and A^* of these diodes were determined from the I–V measurement in the wide temperature range 80–400 K. The temperature dependence of I–V data reveals an increase in BH but a decrease in n with an increase in temperature. Such temperature dependent behavior of BH and n has been interpreted on the basis of TE theory with GD of BHs around a mean value due to BH inhomogeneities prevailing at M/S interface and the A^* of n-Si. Also, the energy distribution profile of N_{ss} of the structure has been obtained from the forward bias I–V data by taking the bias voltage dependence of the effective BH (Φ_e) and n at room temperature.

2. Experimental details

Nickel acetate (0.5 g) and 0.25 g of zinc acetate were mixed with 1 g of polyvinyl alcohol (PVA), molecular

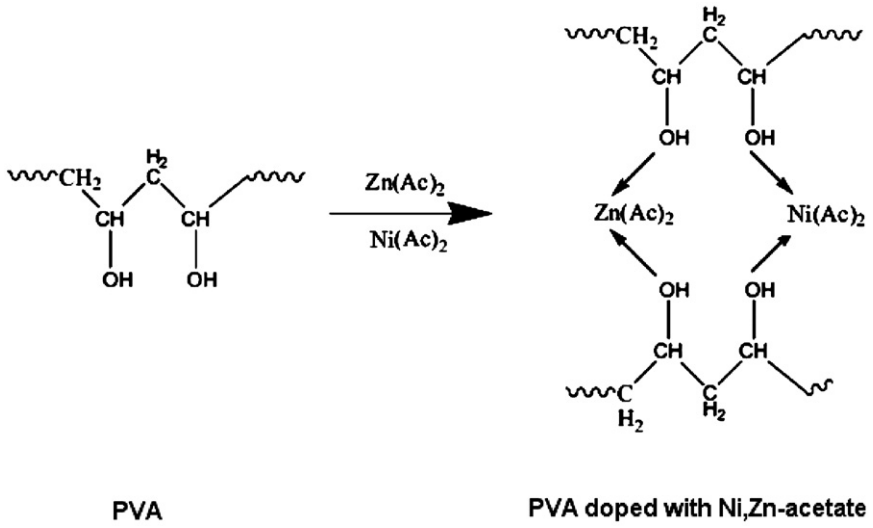

Fig. 1. Chemical structure of PVA, doped with Ni,Zn-acetate.

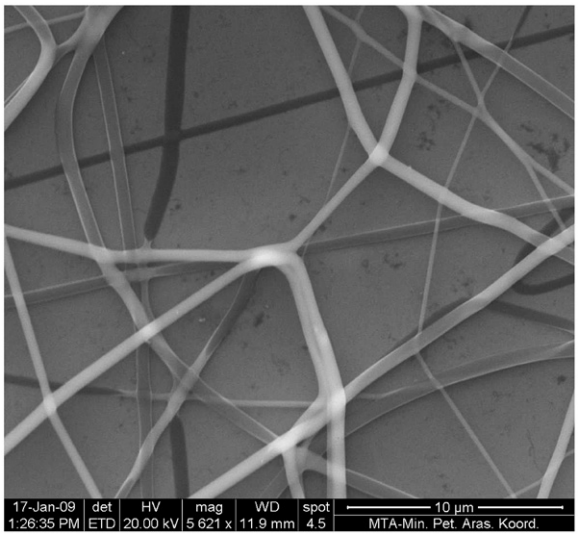

Fig. 2. Selected SEM image of PVA/(Ni,Zn-doped) nanofiber film.

weight=72,000 and 9 ml of deionised water. After vigorous stirring for 2 h at 50 °C, a viscous solution of PVA/(Ni, Zn) acetates was obtained as given in Fig. 1.

PVA (Ni,Zn-doped) nanofiber film on n-Si substrate was coated by electrospinning technique. After spining, the Schottky/rectifier contacts were coated by evaporation with Au dots with a diameter of about 1.0 mm (diode area=7.85×10^{-3} cm^2). The more detailed information about the fabrication of Au/n-Si (1 1 1) SBDs with PVA(Ni,Zn -doped) can be found in our previous study [43].

The temperature dependence of forward bias *I–V* measurements was performed by the use of a Keithley 2400 source meter in the temperature range 80–400 K using a temperature-controlled Janis vpf-475 cryostat, which enabled us to make measurements in the temperature range 77–450 K. The sample temperature was always monitored using a Lake Shore model 321 auto-tuning temperature controllers with sensitivity better than ± 0.1 K. All measurements were carried out with the help of a microcomputer through an IEEE-488 AC/DC converter card. Fiber formation and morphology of the electrospun PVA(Ni,Zn-doped) were determined using a Scanning Electron Microscope (SEM) Quanto 400 FEI MK-2. The diameter of nonwoven fibers was analyzed using ImageJ (Image Processing and Analysis in Java) digital image analysis program. Average PVA(Ni,Zn-doped) fiber diameters were found to be 150 nm. It was also observed that the, PVA (Ni,Zn-doped) nanofibers were highly linear, homogenous and showed no beading (Fig. 2).

3. Results and discussion

For a Schottky diode with a uniform thin interfacial layer and a series resistance, the current through SBD according to the TE theory ($V > 3kT/q$) can be expressed as [17,18]

$$I = I_0 \exp\left(\frac{q(V-IR_s)}{nkT}\right)\left[1-\exp\left(\frac{-q(V-IR_s)}{kT}\right)\right] \quad (1)$$

where V is the applied bias voltage, q is the electronic charge, n is the ideality factor, k is Boltzmann's constant, T is the absolute temperature in Kelvin and I_0 is the reverse saturation current derived from the straight-line intercept of ln I at zero bias and defined by

$$I_0 = AA^*T^2 \exp\left(-\frac{q\Phi_{B0}}{kT}\right) \quad (2)$$

where A is the rectifier contact area, A^* is the effective Richardson constant and is equal to 120 A/cm^{2}K^2 for n-type Si and Φ_{B0} is the apparent barrier height at zero bias, which can be obtained from Eq. (2) as

$$\Phi_{B0} = (kT/q)\ln(AA^*T^2/I_0) \quad (3)$$

The ideality factor, n, is introduced to take into account the deviation of the experimental *I–V* data from the ideal TE theory. From Eq. (1), the value of n can be obtained from the slope of the linear region of the forward bias ln *I–V* plot and can be written as

$$n = \frac{q}{kT}\left[\frac{dV}{d(\ln I)}\right] \quad (4)$$

Fig. 3 shows the forward and reverse bias semi-logarithmic ln *I–V* characteristics of the Au/PVA(Ni,Zn-doped)/n-Si SBD various temperatures, ranging from 80 to 400 K. As it can be seen in Fig. 3, the ln I vs. V plots are

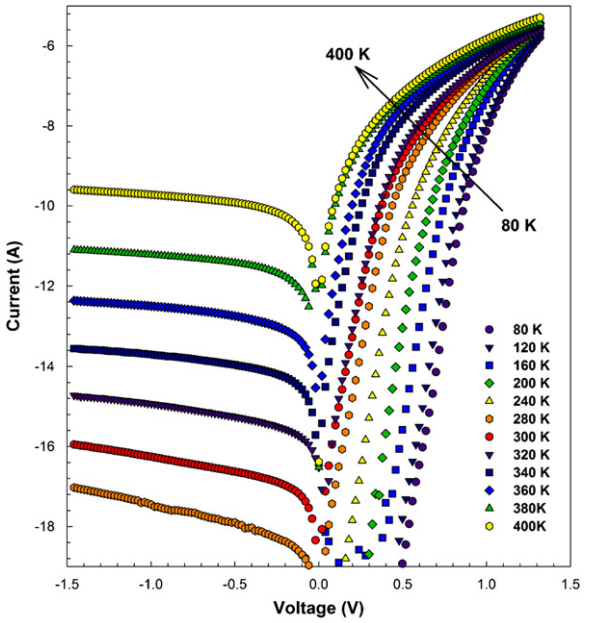

Fig. 3. Forward and reverse bias ln(*I*–*V*) characteristics of the Au/PVA (Ni,Zn-doped)/n-Si structure at various temperatures.

linear between intermediate bias regions ($0.1 \le V \le 0.8$ V). The value of saturation current I_0 has been obtained by extrapolating the linear intermediate bias voltage region of the plot to zero-applied bias voltage for each temperature. The values of Φ_{B0} and n were obtained from Eqs. (3) and (4) for each temperature value, respectively. The obtained experimental values Φ_{B0} and n are reported in Table 1 and Fig. 4. As can be seen, the Φ_{B0} value of 0.78 eV at 300 K obtained for the Au/PVA(Ni,Zn-doped)/n-Si structure is remarkably lower than that achieved with conventional Au/n-Si metal/semiconductor contacts. Sağlam et al. [44] show that the BH obtained from *I*–*V* characteristics for the Au/n-Si Schottky barrier diodes (SBDs) varied from 0.789 to 0.819 eV. As shown in Table 1, the values of Φ_{B0} and n for the Au/PVA(Ni,Zn-doped)/n-Si structure ranged from 0.29 eV and 5.15 (at 80 K) to 0.842 eV and 1.45 (at 400 K), respectively.

Similar results have also been presented by some authors for conventional Au/n-Si SBDs. Sharma [45] fabricated Au/n-Si Schottky barrier diode and reported the Φ_{B0} and n values ranging from 0.79 eV and 1.25 at 310 K to 0.27 eV and 3.53 at 70 K, respectively. Tataroğlu and Altındal [46] fabricated Au/SiO_2/n-Si MIS diode and presented the Φ_{B0} and n values ranging from 0.624 eV and 2.898 (300 K) to 0.794 eV and 1.787 (400 K), respectively. Uğurel et al. [47] fabricated Au/n-Si/Al MS diode and reported the Φ_{B0} and n with values of 0.73 eV and 1.44 at room temperature, respectively.

These high values of n can be attributed to the presence of interfacial PVA layer at M/S interface and particular density distribution on interface states [29,30,34–42]. As explained in Refs. [34–41], since the current transport across the metal–semiconductor interface is a temperature activated process, electrons at low temperatures are able to surmount the lower barriers. Therefore, the current transport will be dominated by the current flowing through the patches of lower barriers. Hence, the temperature dependent value of n increases with the decreasing temperature. In addition, as shown in Fig. 4, Φ_{B0} values show an unusual behavior that they increase with the increasing temperature. Such temperature dependence of Φ_{B0} is an obvious disagreement with the reported the negative temperature coefficient of the barrier height or forbidden band gap of Si, which is attributed to the highly polar nature of PVA. In addition, it is well known that the value of energy band gap of the semiconductor changes with temperature according to the following equation [17,18]:

$$E_g(T) = E_g(0) + \frac{\alpha T^2}{(\beta + T)} \tag{5a}$$

Table 1
Temperature dependent values of various parameters determined from the forward bias *I*–*V* characteristics of the Au/PVA(Ni,Zn-doped)/n-Si structure.

T (K)	I_0 (A)	n	Φ_{B0} (eV)
80	8.08×10^{-15}	5.150	0.290
120	2.06×10^{-14}	3.600	0.434
160	8.26×10^{-13}	2.894	0.540
200	1.55×10^{-12}	2.340	0.667
240	9.81×10^{-11}	2.130	0.722
280	3.5×10^{-9}	1.960	0.763
300	2.10×10^{-8}	1.830	0.780
320	3.90×10^{-8}	1.690	0.810
340	2.10×10^{-7}	1.600	0.820
360	7.43×10^{-7}	1.530	0.831
400	9.64×10^{-6}	1.450	0.842

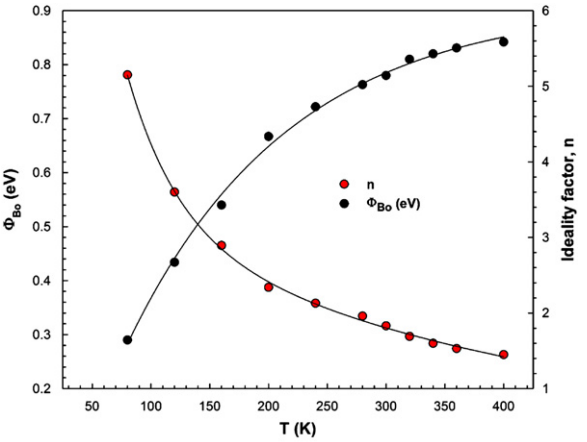

Fig. 4. Φ_{B0} and n of the Au/PVA(Ni,Zn-doped)/n-Si structure at various temperatures.

where α and β are the temperature coefficient of energy band gap of the semiconductor and a constant, respectively. Their values are $\alpha = -4.73 \times 10^{-4}$ eV/K and β=636 for Si. Therefore, the values of Φ_{B0} and BH must be changed similarly with temperature as

$$\Phi_B(T) = \Phi_B(0) + \alpha T \tag{5b}$$

where $\Phi_B(0)$ and α are the barrier height at absolute temperature and temperature coefficient of barrier height. In our calculations the values of α are positive contrary to temperature coefficient of forbidden bandgap for Si.

As shown in Fig. 5, the ideality factor varies almost linearly with the inverse temperature as

$$n(T) = n_0 + T_0/T \tag{6}$$

where n_0 and T_0 are constants, which were found to be 0.558 and 367.65 K, respectively.

In order to evaluate the Φ_{B0}, one might also use the conventional activation energy plot of the reverse saturation current I_0. Therefore, Eq. (2) can be rewritten as

$$\ln\left(\frac{I_0}{T^2}\right) = \ln(AA^*) - \frac{q\Phi_{B0}}{kT} \tag{7}$$

Fig. 6 shows the conventional Richardson plot of $\ln(I_0/T^2)$ vs. q/kT for the Au/PVA(Ni,Zn-doped)/n-Si SBD at various temperatures. This plot should yield a straight line with a slope and intercept, which correspond to the Φ_{B0} and A^*, respectively.

In order to investigate the temperature dependence of the ideality factor (n), we plotted n vs. $1/T$ (Fig. 5). As shown in Fig. 5, at high temperatures, the value of n is closer to unity (ideal case), while at low

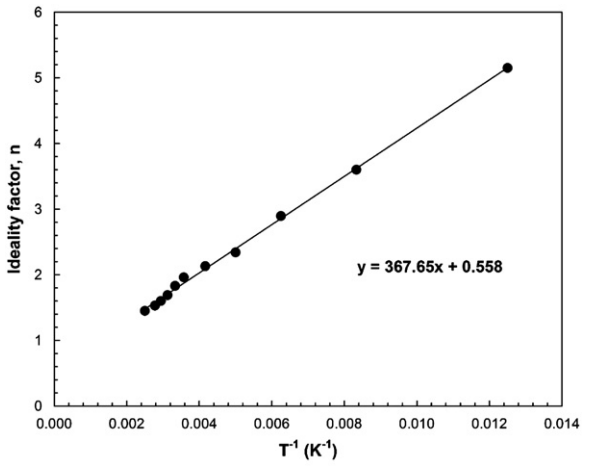

Fig. 5. Plot of n–T^{-1} of the Au/PVA(Ni,Zn-doped)/n-Si structure at various temperatures.

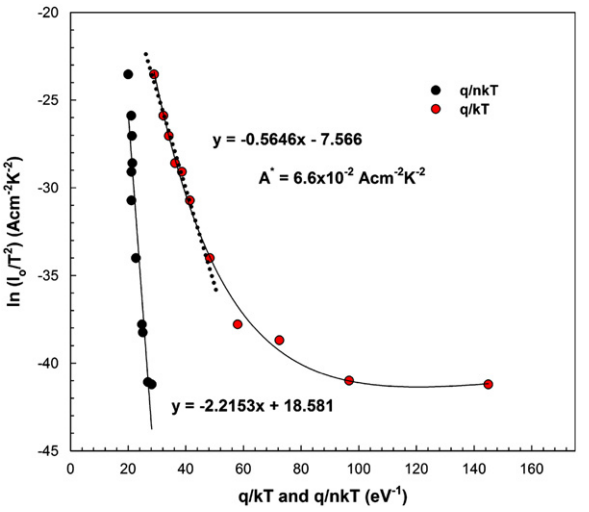

Fig. 6. Richardson plots of the $\ln(I_0/T^2)$ vs. q/kT or q/nkT for the Au/PVA(Ni,Zn-doped)/n-Si structure at various temperatures.

temperatures, n increases with decreasing temperature. Such behavior of n may be described as the "T_0 anomaly or effect". The other reason for such temperature dependence of n could be attributed to the inhomogeneities of the SBH [27,48,49]. Furthermore, the values of n are not constant with temperature, and they are observed to change linearly with the inverse temperature ($1/T$), as can be seen in Fig. 5. Consequently, the experimental results reveal an abnormal increase in the Φ_{B0} and a decrease in the n with temperature, and leads to non-linearity in the conventional Richardson plot of $\ln(I_0/T^2)$ vs. q/kT (Fig.6). However, the $\ln(I_0/T^2)$ vs. q/nkT plot is linear in the whole temperature range. Similar results have been observed by Pakma et al. [27], Yıldırım et al. [48] and Aydın et al. [49]. The values of activation energy ($E_a = \Phi_{B0}$) and Richardson constant (A^*) in this temperature range were obtained as 0.56 eV and 6.6×10^{-2} Acm^{-2} K^{-2}, respectively. The A^* values are much lower than the known value of 120 Acm^{-2} K^{-2} for n-type Si [17,18]. In addition, especially the value of 0.56 eV obtained from the slope of $\ln(I_0/T^2)$ vs. $1/T$ plot is almost equal to half of the energy band gap of Si. These results confirm that the predominant current-conduction mechanism is not only the TE. The tail to the abscissa in Fig. 6 was caused by the temperature dependence of the Φ_{B0} and n. The deviation in the Richardson constant may be explained by spatial inhomogeneous barrier heights and potential fluctuations at the interface consisting of low and high barrier areas [29,30,50].

According to Tung's [51] theoretical approach, there is a linear correlation between the experimental Φ_{B0} and n. Horvath [50] has explained that the A^* value may be affected by the lateral inhomogeneity of the barrier. In addition, Song et al. [52] has suggested that the contact area A is composed of many sub-areas, each having a definite Φ_{B0} and a definite area being isolated from each other. They show that in the Schottky diodes variations of the Φ_{B0} over the contact area can occur as a result of inhomogeneities in the interfacial layer composition, non-uniformity of the interfacial layer thickness and distributions of interfacial charges. Fig. 7 shows a plot of experimental Φ_{B0} vs. n for various temperatures. As it can be seen in Fig. 7, there is a linear relationship between the Φ_{B0} and n, which has been explained by lateral inhomogeneities of the BHs in the Au/PVA(Ni,Zn-doped)/n-Si SBD. The extrapolation of the Φ_{B0} vs. n plot to $n=1$ has given a homogeneous Φ_{B0} of approximately 0.903 eV. Thus, it can be said that the significant decrease of the zero-bias Φ_{B0} and increase of n especially at low temperatures are possibly caused by the Φ_{B0} inhomogeneities.

The GD of the BHs with a mean value $\overline{\Phi}_{B0}$ and standard deviation σ_0 yields the following expression of the BH [31–41,50–52]:

$$\Phi_{ap} = \overline{\Phi}_{B0}(T=0) - \frac{q\sigma_0^2}{2kT} \tag{8}$$

where the temperature dependence of σ_0 is usually small and can be neglected [29,30,34–42]. The observed variation of ideality factor with

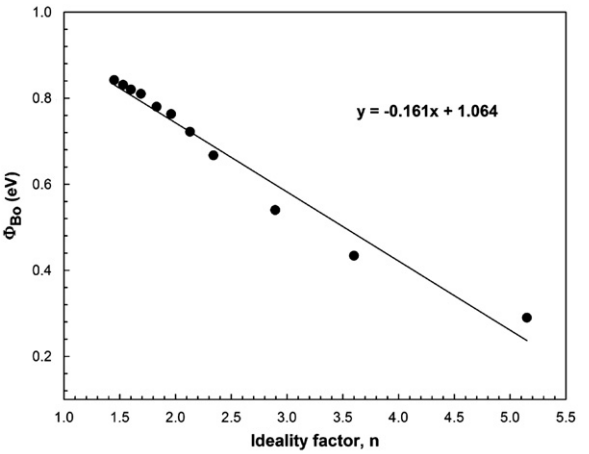

Fig. 7. Temperature dependent experimental Φ_{B0} vs. n plot for the Au/PVA(Ni,Zn-doped)/n-Si structure.

temperature in the model is given by [34–40,50–52]

$$\left(\frac{1}{n_{ap}} - 1\right) = \rho_2 - \frac{q\rho_3}{2kT} \tag{9}$$

where n_{ap} is the apparent ideality factor and ρ_2 and ρ_3 are voltage coefficients, which may depend on temperature, quantifying the voltage deformation of the BH distribution [50–53]. Therefore, we have attempted to draw a Φ_{B0} vs. $q/2kT$ plot (Fig. 8) to obtain evidence of a Gaussian distribution of the BH, and the values of $\overline{\Phi}_{B0}$=0.974 eV and σ_0=0.101 V for the mean barrier height and standard deviation at zero bias, respectively, were obtained from this plot. It was found that the value of σ_0=0.101 V is not small compared to the mean value of $\overline{\Phi}_{B0} = 0.974$ eV, and it indicates the presence of the interface inhomogeneities. Also, as it can be seen from Fig. 8, the plot of $((1/n_{ap})-1)$ vs. $q/2kT$ gives a straight line. Similarly, it is possible to see from Fig. 8 that the value of ρ_2 obtained from the intercept of the experimental n_{ap} vs. $q/2kT$ plot is -0.215 and the value of ρ_3 from the slope is -0.011 V. These results indicate the presence of a single Gaussian distribution of BH in the Schottky contact area. Now, the conventional Richardson plot

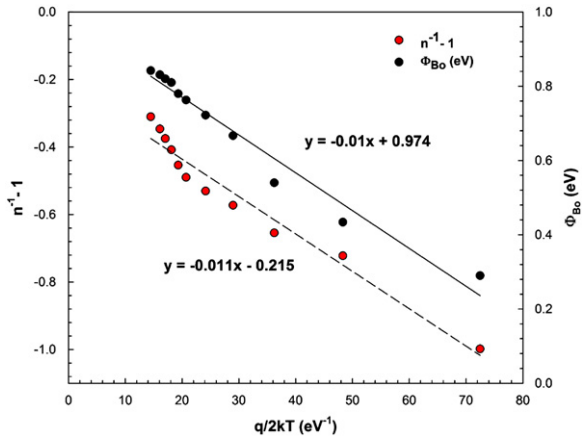

Fig. 8. Apparent Φ_{B0} and n vs. $q/2\,kT$ plots of the Au/PVA(Ni,Zn-doped)/n-Si structure at various temperatures.

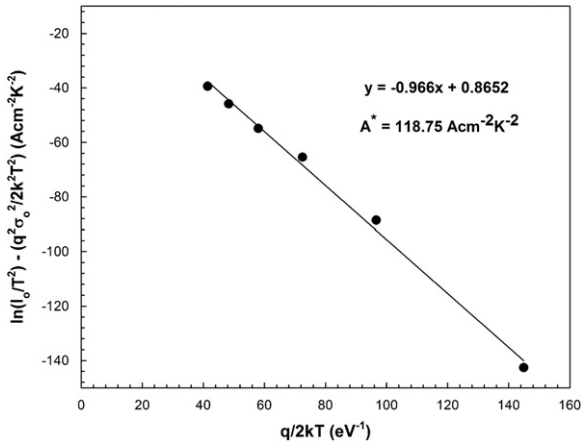

Fig. 9. Modified activation energy plot for the Au/PVA(Ni,Zn-doped)/n-Si structure at various temperatures.

can be modified by combining with Eqs. (2) and (7) as follows:

$$\ln\left(\frac{I_0}{T^2}\right)-\left(\frac{q^2\sigma_0^2}{2k^2T^2}\right)=\ln(AA^*)-q\frac{\overline{\Phi}_{B0}}{kT} \tag{10}$$

Thus, the plot of a modified activation energy plot according to Eq. (10) should give a straight line with the slope, which directly yields the mean $\overline{\Phi}_{B0}$ as 0.966 eV and the intercept ($=\ln AA^*$) at the ordinate such that A^* for a given diode area A was determined as 118.75 A/cm^{2}K^2 (Fig. 9), respectively, without using the temperature coefficient of the SBHs. It is clear that the value of $\overline{\Phi}_{B0}=0.966$ eV obtained from the modified activation energy plot (according to Eq. (10)), is in agreement with the value of $\overline{\Phi}_{B0}=0.974$ eV from Φ_{ap} vs. $q/2kT$ (according to Eq. (8)). Hence, it has been concluded that the temperature dependence of the forward I–V characteristics of the Au/PVA(Ni,Zn-doped)/n-Si structure can be successfully explained on the basis of TE mechanism with a GD of BH.

4. Conclusions

The forward and reverse bias I–V characteristics of the Au/PVA(Ni,Zn-doped)/n-Si structure have been measured in the temperature range 80–400 K. Using the evaluation of the experimental forward bias I–V data based on TE theory reveals an increase in Φ_{B0} and a decrease in the n with the increasing temperature and these changes are quite significant at low temperatures. Temperature dependence behavior of Φ_{B0} (I–V) and n is attributed to the Schottky barrier inhomogeneities by assuming a GD of BH due to barrier inhomogeneities that prevail at M/S interface. Therefore, we drew Φ_{B0} vs. $q/2kT$ plot, and the values of $\overline{\Phi}_{B0}$ and standard deviation at zero bias (σ_0) were obtained from this plot as 0.974 eV and 0.101 V, respectively. Thus, modified $\ln(I_0/T^2)-q^2\sigma_0^2/2(kT)^2$ vs. q/kT plot gives the values of $\overline{\Phi}_{B0}$ and Richardson constant A^* as 0.966 eV and 118.75 A/cm^{2}K^2, respectively. This value of the A^* (=118.75 A/cm^2 K^2) is very close to the theoretical value of 120 A cm^{-2} K^{-2} for n-type Si.

Acknowledgements

This work is supported by Gazi University Scientific Research Project numbered 04/2010-27.

References

[1] Tsunoda S, Koezuka H, Kurata T, Yanaura S, Ando T. J Polym Sci B 1988;2:1697.
[2] Gupta RK, Singh RA. Mater Chem Phys 2004;86:279.
[3] Gupta RK, Singh RA. Compos Sci Technol 2005;65:677.
[4] Yakuphanoğlu F. Synth Met 2008;158:108.
[5] Akkılıç K, Yakuphanoğlu F. Microelectron Eng 2008;85:1826.
[6] Rajesh RK, Menon SC. J Non-Cryst Solids 2007;353:398.
[7] Nguyen CV, Potje-Kamloth K. Thin Solid Films 1999;338:142.
[8] Aydoğan Ş, Sağlam M, Türüt A. Polymer 2005;46:563.
[9] Li-Ming Huang, Ten-Chin Wen, Gopalan A. Thin Solid Films 2005;473:300.
[10] Çakar M, Biber M, Sağlam M, Türüt A. J Polym Sci B 2003;41:1334.
[11] Dökme İ, Altındal Ş, Bülbül MM. Appl Surf Sci 2006;252:7749.
[12] Temirci C, Çakar M, Türüt A, Onganer Y. Phys Status Solidi (a) 2004;201:3077.
[13] Aydin ME, Kiliçoğlu T, Akkiliç K, Hoşgören H. Physica B 2006;381:113.
[14] Tagmouti S, Outzourhit A, Oueriagli A, Khaidar M, Elyacoubi M, Evrard R, et al. Sol Energy Mater Sol Cells 2002;71:9.
[15] Akkiliç K, Uzun İ, Kiliçoğlu T. Synth Met 2007;157:297.
[16] Bohler A, Dirr S, Johannes HH, Ammermann D, Kowalsky W. Synth Met 1997;91:95.
[17] Sze SM. Physics of Semiconductor Devices. New York: Wiley; 1981 p. 850.
[18] Rhoderick EH, Williams RH. Metal Semiconductor Contacts. 2nd ed.. Oxford: Clarendon Press; 1988.
[19] Sheap A, Abd. Allah RA, Basha AF, Abdel-Kader FH. J Appl Polym Sci 1998;68:687.
[20] Uma Devi C, Sharma AK, Rao VVRN. Mater Lett 2002;56:167.
[21] Kumar GV, Chandramani R. Acta Phys Pol A 2010;117:917.
[22] Bülbül MM, Bengi S, Dökme İ, Altındal Ş, Tunç T. J Appl Phys 2010;108:034517.
[23] Kampen T, Schuller A, Zahn DRT, Biel B, Ortega J, Perez R, et al. Appl Surf Sci 2004;234:341.
[24] Bhajantri RF, Ravindrachary V, Harisha A, Ranganathaiah C, Kumaraswamy GN. Appl Phys A 2007;87:797.
[25] Hoffman A. Ann NY Acad. Sci. 2001;62:944.
[26] Subba Reddy ChV, Han X, Zhu QY, Mai LQ, Chen W. Microelectron Eng 2006;83:281.
[27] Pakma O, Serin N, Serin T, Altındal Ş. J Appl Phys 2008;104:014501.
[28] Arslan E, Altındal Ş, Özçelik S, Ozbay E. J Appl Phys 2009;105:023705.
[29] Karataş Ş, Altindal Ş, Türüt A, Özmen A. Appl Surf Sci 2003;217:250.
[30] Zeyrek S, Altindal Ş, Yüzer H, Bülbül MM. Appl Surf Sci 2006;252:2999.
[31] Norde H. J Appl Phys 1979;50:5052.
[32] Sato K, Yasamura YJ. Appl Phys 1985;58:3655.
[33] Cheung SK, Cheung NW. Appl Phys Lett 1986;49:85.
[34] Gümüs A, Türüt A, Yalçin N. J Appl Phys 2002;91:245.
[35] Werner JH, Guttler HH. J Appl Phys 1991;69:1552.

[36] Chand S, Bala S. Appl Surf Sci 2005;252:358.
[37] Chand S, Kumar J. Semicond Sci Technol 1996;11(1):1203.
[38] Chand S, Kumar J. Appl Phys A 1997;65:497.
[39] Sağlam M, Biber M, Türüt A, Ağırtaş MS, Çakar M. Int J Polym Mater 2005;54:805.
[40] Zhu S, Van Meirhaeghe RL, Detavernier C, Cardon F, Ru GP, Qu XP, et al. Solid-State Electron 2000;44:663.
[41] Sullivan JP, Tung RT, Pinto MR, Graham WR. J Appl Phys 1991;70:7403.
[42] Card HC, Rhoderick EH. J Phys D: Appl Phys 1971;4:1589.
[43] Dökme İ, Altındal Ş, Tunç T, Uslu İ. Microelectron Reliab 2010;50:39.
[44] Sağlam M, Cimilli FE, Türüt A. Physica B 2004;348:397.
[45] Sharma R. J Electron Devices 2010;8:286.
[46] Tataroğlu A, Altındal Ş. J Alloys Compd 2009;479:893.
[47] Uğurel E, Aydoğan Ş, Şerifoğlu K, Türüt A. Microelectron Eng 2008;85:2299.
[48] Yildirim N, Korkut H, Türüt A. Eur Phys J Appl Phys 2009;45:10302.
[49] Aydın ME, Yildirim N, Türüt A. J Appl Phys 2007;102:043701.
[50] Horvarth Zs J. Solid-State Electron 1996;39:176.
[51] Tung RT. Phys Rev B 1992;45:13509.
[52] Song YP, Van Meirhaeghe RL, Laflere WH, Cardon F. Solid-State Electron 1986;29:633.
[53] Zhu S, Detavernier C, Van Meirhaeghe RL, Cardon F, Ru GP, Qu XP, et al. Solid-State Electron 2000;44:1807.